Use of transmission electron microscopy in the characterization of GaInNAs(Sb) quantum well structures grown by molecular beam epitaxy

Tihomir Gugov,[a] Vincent Gambin, Mark Wistey, Homan Yuen, Seth Bank, and James S. Harris, Jr.
Solid State and Photonics Laboratory, Stanford University, Stanford, California 94305

(Received 27 October 2003; accepted 30 December 2003; published 9 June 2004)

The quaternary GaInNAs alloy is a very promising material system for lasers in the 1.2–1.6 μm range with application in telecommunication fiber-optic networks. While good quality laser material has been demonstrated at 1.3 μm, pushing the emission beyond 1.5 μm by adding up to 40% In and 2% N has been unsuccessful. Recently, the addition of small amounts of Sb has put this alloy back on track for the 1.5 μm challenge by dramatically improving the luminescence efficiency of the material. In this work, high-resolution transmission electron microscopy (TEM), energy-filtered TEM, dark-field TEM, and energy-dispersive x-ray spectroscopy were used to structurally characterize both GaInNAs and GaInNAsSb quantum well structures. The results provide insight into the role of antimony in improving the optical properties of the material, namely reducing the local compositional fluctuations of In. © *2004 American Vacuum Society.*
[DOI: 10.1116/1.1650853]

I. INTRODUCTION

The ever increasing demand for faster (gigabit) metro and local area networks has spurred great interest in the GaInNAs(Sb) material system in recent years. Optical sources based on GaInNAs(Sb) emit light in the 1.3–1.55 μm range, which makes them ideally suited for telecommunication applications. Moreover, edge-emitting and vertical cavity surface emitting lasers based on this material offer a low cost alternative to the InGaAsP/InP Bragg grating and distributed feedback lasers currently used in fiber-optic networks. The low cost advantage of GaInNAs(Sb) lasers stems from the fact that this material can be grown on GaAs substrates, an inexpensive and well-developed technology. In addition, due to the large conduction band offset intrinsic to this system, these lasers have very good thermal performance and can operate essentially uncooled. Another intended application of this material is in high power lasers that are to serve as pumps in Raman amplifiers.

While the earlier mentioned characteristics make GaInNAs(Sb) an excellent candidate for laser material, significant growth challenges have to be overcome before its potential can be realized. This alloy is characterized by a large miscibility gap which requires that it be grown at low temperatures in metastable regimes. A lot of the growth challenges have been addressed for 1.3 μm emission alloy (containing up to 30% In and 2% N) and several groups[1–4] have been successful in fabricating lasers at this wavelength. The effort to push emission to 1.55 μm, which requires compositions of up to 40% In, has proven next to impossible due to the tendency of the material to phase segregate in this high In concentration regime.[5] Very recently, the addition of a small amount of Sb has put the race for 1.55 μm material back on track by dramatically improving the optical properties of the alloy.[6–8]

This study presents the use of transmission electron microscopy (TEM) as a powerful tool in the effort to understand the role of Sb in improving the material quality. Researchers in this area have long suspected that local compositional fluctuations are responsible for the broad emission spectra, low gain, and high threshold currents of lasers based on this material. We employ several different TEM techniques to probe the local atomic structure of the alloy and investigate whether these fluctuations do indeed occur.

II. EXPERIMENT

In this work, both GaInNAs and GaInNAsSb samples were investigated. Structures containing either one or three quantum wells (QWs) were grown by solid source molecular beam epitaxy on GaAs substrates. All QWs had an 8 nm nominal thickness, with 20 nm barriers in between. GaInNAs samples had a nominal composition of 30% In and 1.6% N. GaInNAsSb samples had a nominal composition of 38% In, 1.6% N, and 2% Sb in the wells and 2.3% N and 6% Sb in the GaNAsSb barriers. The substrate temperature was kept low during growth at around 420 °C to prevent phase segregation. Arsenic and antimony were supplied in thermally cracked form and atomic nitrogen was generated from a radio frequency (rf) plasma source. The rf power was 300 W and the nitrogen flow rate was maintained constant at 0.5 sccm.

Cross-sectional TEM samples were prepared in the (110) orientation using the "sandwich" technique. All samples were in the as-grown condition (i.e., not annealed). Thinning was achieved by grinding and polishing followed by 5 keV Ar^+ ion milling at low angles to achieve electron transparency. A final polishing 1 keV low temperature ion milling was performed to achieve very smooth surfaces.

[a]Author to whom correspondence should be addressed; electronic mail: tgugov@stanford.edu

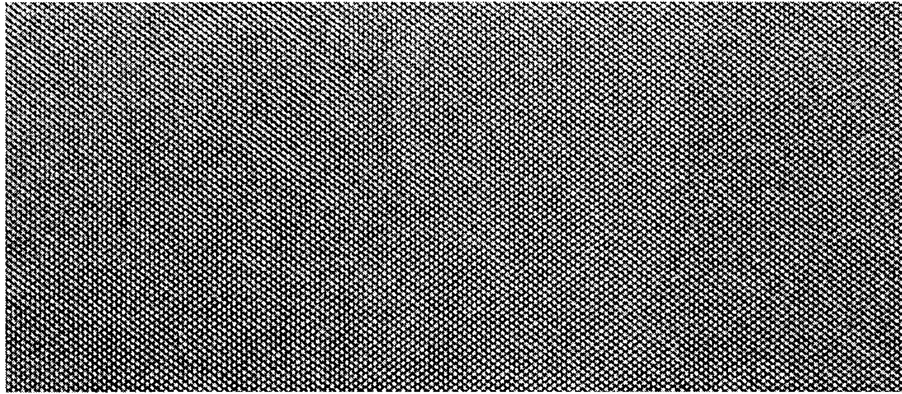

a.

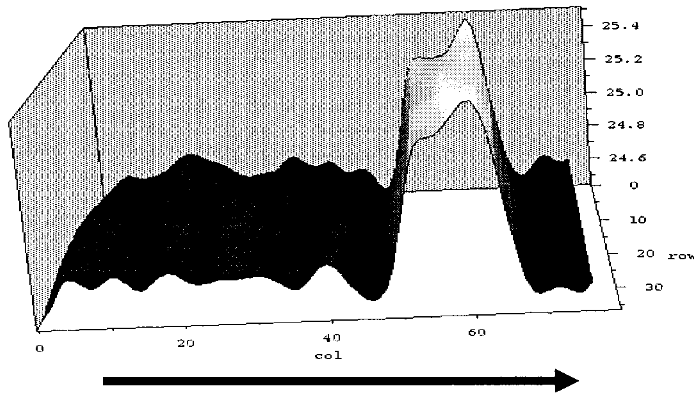

Surface

FIG. 1. HRTEM image of the QW area of a GaInNAs sample (a) and strain map across the well (b).

High-resolution TEM (HRTEM) lattice images of the QWs area were obtained in a 800 kV, 0.15 nm resolution JEOL microscope and recorded on photographic plates. Energy-filtered TEM (EFTEM) images and energy-dispersive x-ray (EDX) spectra were obtained in a Philips CM-200 microscope equipped with Gatan GIF analyzer, Oxford energy dispersive spectra detector, scanning TEM annular detector and CCD camera with 1024×1024 pixels. Dark-field (DF) images with the chemically sensitive (002) reflection were also obtained on the CM-200 machine.

Strain maps were generated from the high resolution lattice images using the DARIP program developed at the National Center for Electron Microscopy (NCEM) at the Lawrence Berkeley National Laboratory (LBNL) in Berkeley, California. EFTEM images were analyzed with Digital Micrograph, a commercial image processing software available from Gatan, Inc.

III. RESULTS AND DISCUSSION

Figure 1 shows a selection from a HRTEM lattice image of the quantum well area of a GaInNAs sample (a) and the corresponding strain map across the well (b). The image was taken in the [110] zone axis. Performing strain mapping analysis requires very high quality lattice images over large areas of the sample. Therefore, it is critical to perform a final very low energy (1 keV) ion polishing on the sample to achieve very smooth surfaces and large thin areas. Strain mapping analysis is further complicated by the fact that strained layers, such as quantum wells, tend to relax when the sample becomes very thin. A good rule of thumb is that the sample area analyzed in the TEM should be several times thicker than the QW in order to avoid relaxation. This is the main reason why we chose an 800 kV machine for the HRTEM images. With this high energy beam, thicker areas of the sample are still transparent to the electrons and can be analyzed.

Strain mapping is performed on the HRTEM images in several steps. First, the images are filtered to subtract the diffuse background intensity and make the peaks (which can be interpreted as the positions of the atoms) more defined. Then, the DARIP program is used to identify and mark those peaks. Next, a lattice is defined by choosing several peaks and based on this, DARIP calculates a lattice which it locks to these peak positions. The data are then extracted and a strain map is generated, which is essentially a map of the lattice parameter over the selected area. Figure 1(b) shows this type of strain map for a single QW GaInNAs sample. The well clearly appears as a peak due to the fact that In swells the lattice, being a larger atom than Ga; the higher the In concentration, the greater the lattice distortion. Figure 1(a) shows clearly that the In concentration profile is very asymmetric. It consists of two bumps with the higher In concen-

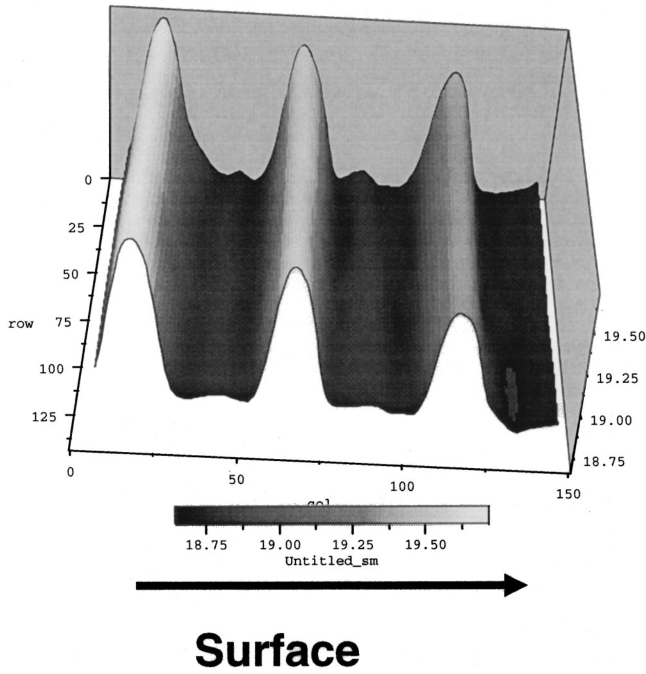

FIG. 2. Strain map across a three QW GaInNAsSb sample.

tration occurring near the top interface of the well, providing evidence that In segregates near the top of the well. This is very undesirable since there are effectively two different In compositions in the well, which would broaden the emission spectrum. The difference in the rear and leading edge compositions was estimated to be around 8%.

Figure 2 shows the strain map across the three QWs in a GaInNAsSb sample. The compositional profiles across the wells appear very uniform due to the antimony. The peak height decreases from the bottom to the top well, which likely indicates decreased In incorporation. The variation of In concentration between the wells is roughly 4%. This confirms the suspicion that some heating occurs during subsequent well growth. The wells have a smaller band gap than the GaAs substrate and absorb more heat, which effectively raises the growth temperature and leads to a decreased In incorporation. Another possibility is that strain accumulates with an increasing number of wells (especially if the barriers are not under tensile strain to provide strain compensation) which would also decrease In incorporation. It is clear that growth adjustments would be necessary to counteract these effects.

Figure 3 shows extended strain maps along each of the wells of the GaInNAsSb sample in order to examine the compositional uniformity within the wells. It should be emphasized again that overall these appear much more uniform than the GaInNAs QW, due to the Sb. Figure 3 shows that the uniformity deteriorates somewhat from the bottom to the top well. The last well shows some In clustering with a segregation distance of 20–30 nm, but this is not nearly as severe as with GaInNAs. This is probably due to the same effects described earlier, namely heating and strain accumulation during growth which promote phase segregation.

Figure 4 shows an EFTEM image of the GaInNAsSb sample (a) and the corresponding intensity profile across the wells (b). The image is formed by selecting only the electrons that are scattered inelastically off the In atoms, so the wells where In is concentrated appear as very bright stripes. The contrast within the wells appears rather uniform which confirms that there is no significant In clustering. The intensity profile reveals the same trend as the strain maps, namely

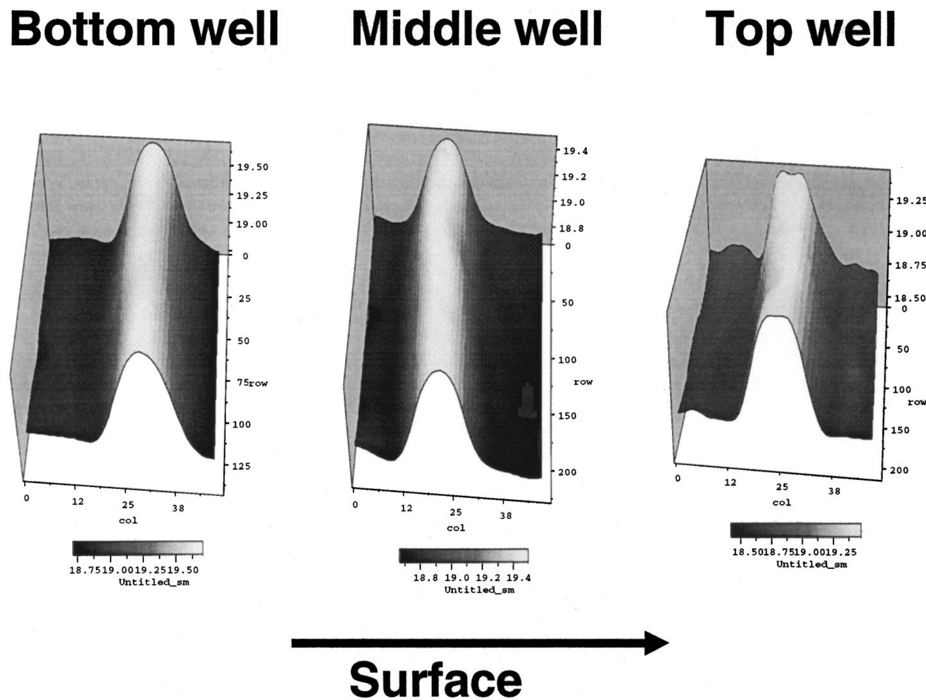

FIG. 3. Extended strain maps along each of the wells of the GaInNAsSb sample.

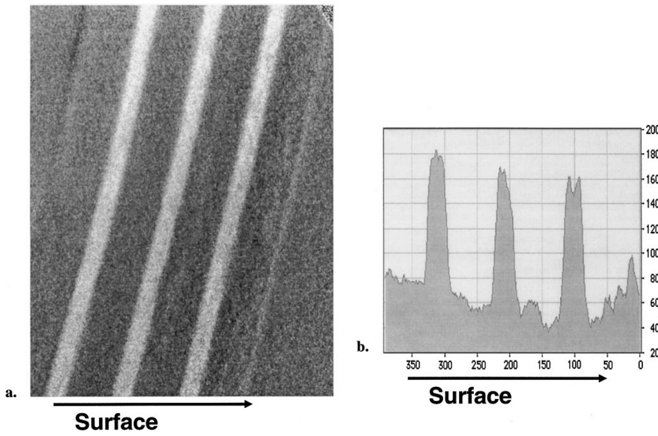

FIG. 4. EFTEM image of the GaInNAsSb sample (a) with corresponding intensity profile across the wells (b).

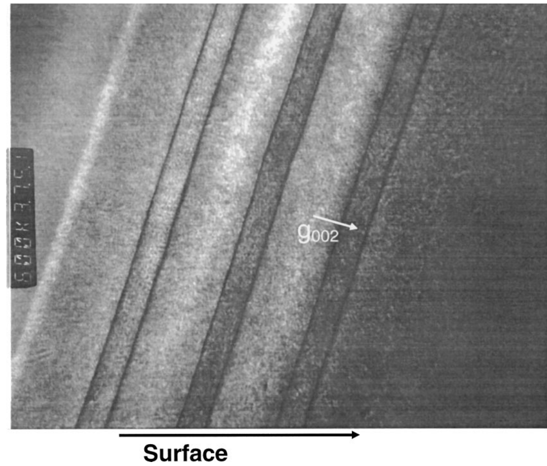

FIG. 6. DF image with the chemically sensitive (002) reflection.

the decrease in the In concentration from the bottom to the top well.

Figure 5(a) presents an EDX profile (In and Sb signals) across the GaInNAsSb sample. It reveals the same trend of decreasing indium concentration towards the surface, although the decrease is not as dramatic as revealed by the strain map. Figure 5(b) shows the EDX profile (In signal) for the GaInNAs sample. Although the profile is broadened due to the poor resolution of the EDX technique (around 2 nm), it shows some evidence of In segregation near the top surface of the well, which is in agreement with the GaInNAs QW strain map.

Figure 6 shows a dark-field (DF) image which was taken with the chemically sensitive (002) reflection. The intensity of the (002) reflection has a square dependence on the difference between the composite structure factors of the group III and group V atoms and for the GaInNAs alloy is modeled as follows:[9,10]

$$I_{002}=A^2=k^2|f_{\mathrm{III}}-f_{\mathrm{V}}|^2,$$

$$f_{\mathrm{III}}=x(f_{\mathrm{In}}-f_{\mathrm{Ga}})+f_{\mathrm{Ga}},$$

$$f_{\mathrm{V}}=y(f_{\mathrm{N}}-f_{\mathrm{As}})+f_{\mathrm{As}},$$

where I_{002} is the (002) intensity, f designates the structure factors, x and y are the fractions of In and N, respectively, and k is a constant. In Fig. 6, the wells show up as stripes clearly delineated by dark lines. These occur at the well interfaces because the combination of the fractions x and y are such that the reflection is completely extinguished. Within the wells, as the In concentration increases, the (002) reflection is no longer extinguished and the brightness is recovered. Thus, a higher In concentration will result in increased brightness. Figure 6 shows a trend of decreased well brightness towards the surface, which is again in agreement with the findings of the other TEM techniques of decreased In incorporation for successive wells.

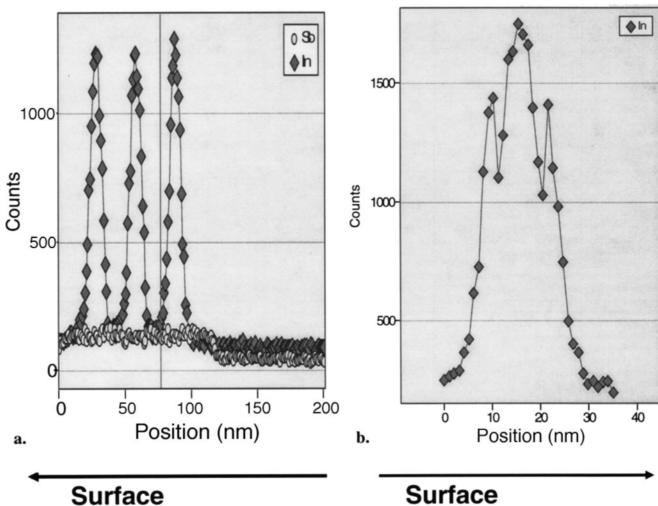

FIG. 5. EDX profile across GaInNAsSb sample (a) and GaInNAs sample (b).

IV. CONCLUSION

In this study, four different TEM techniques were used to structurally characterize GaInNAs and GaInNAsSb QW structures. Strain maps generated from HRTEM images revealed that: (1) Sb dramatically improves compositional uniformity within the wells and (2) In concentration decreases during subsequent well growth. EFTEM, EDX, and DF imaging verified the findings from the strain maps. The results provide insight into the role of Sb in improving the optical properties of the material, namely preventing the segregation of In. Adjustments to the growth conditions are necessary to prevent the drop in indium concentration during growth.

ACKNOWLEDGMENTS

The authors would like to thank Christian Kisielowski, Cheng Yu Song, and Alfredo Tolley at NCEM at LBNL and Kerstin Volz for their valuable help and advice with all aspects of the TEM analysis. They acknowledge DARPA/ONR Optoelectronics Materials Center (Contract No. MDA 972-00-1-0024 and ONR (Contract No. N00014-01-1-0010) for financially supporting this work. T.G. acknowledges the Stanford Graduate Fellowship for supporting his studies at Stanford.

[1]S. Sato, Y. Osawa, T. Saitoh, and I. Fujimura, Electron. Lett. **33**, 1386 (1997).
[2]J. S. Harris, IEEE J. Sel. Top. Quantum Electron. **6**, 1145 (2000).
[3]A. Wagner *et al.*, Appl. Phys. Lett. **76**, 271 (2000).
[4]A. Ramakrishnan, G. Steinle, D. Supper, C. Degen, and G. Ebbinghaus, Electron. Lett. **38**, 322 (2002).
[5]K. Volz, A. K. Schaper, A. Hasse, T. Weirich, F. Höhnsdorf, J. Koch, and W. Stolz, Mater. Res. Soc. Symp. Proc. **619**, 291 (2000).
[6]S. Bank, W. Ha, V. Gambin, M. Wistey, H. Yuen, L. Goddard, S. Kim, and J. S. Harris, J. Cryst. Growth **251**, 367 (2003).
[7]S. Bank, M. Wistey, W. Ha, H. Yuen, L. Goddard, and J. S. Harris, Electron. Lett. **39**, 1445 (2003).
[8]J. S. Harris, Jr., Semicond. Sci. Technol. **17**, 880 (2002).
[9]M. Albrecht *et al.*, Appl. Phys. Lett. **81**, 2719 (2002).
[10]J.-M. Chauveau, A. Trampert, M.-A. Pinault, E. Tournie, K. Du, and K. Ploog, J. Cryst. Growth **251**, 383 (2003).